Oligothiophene Catenanes and Knots. Part II. Mono and Dications. A Theoretical Study

Serguei Fomine,* Patricia Guadarrama, and Paola Flores

*Instituto de Investigaciones en Materiales, Universidad Nacional Autónoma de México,
Apartado Postal 70-360, CU, Coyoacán, México DF 04510, México*

Received: November 22, 2006; In Final Form: February 26, 2007

Mono- and dications of catenanes and knots containing 16, 22, and 28 thiophene units have been studied at the BHandHLYP/3-21G* level of theory. The polaron localization and relaxation energies of monoionized molecules increase with dihedral angle between thiophene fragments, being higher for catenanes and knots compared to linear oligomers. Monoionization of catenanes results in the polaron localization at one macrocycle leaving another one intact. In all diionized oligomers, polaron pairs were found to be more stable than corresponding bipolarons. The energy difference between bipolaron and polaron pairs increases with the number of repeating units in oligomers for all studied molecular architectures. Singlet polaron pairs are more stable than triplet ones. The energy difference between triplet and singlet states does not exceed 7−8 kcal/mol and decreases with the number of thiophene units in oligomers. Two different singlet minima were found for diionized catenanes. In the first one (the most stable), each macrocycle loses one electron, and in the other one, the polaron pairs are located at one macrocycle, leaving another intact. The energy difference between two minima decreases with the number of repeating units in catenanes.

Introduction

Exploitation of non conventional geometry is an excellent tool to tune electronic and other physical properties of conjugated polymers. Thus, it has been observed that supramolecular assemblies of regioregular polyalkylthiophenes have a two-dimensional well-organized lamellar structure[1] with reduced interchain separation (3.7−3.8 Å (thiophene ring-stacking)). The mobility of positive carriers increases with respect to typical values.[2] The absorption spectrum is red-shifted, indicating an increase of the average conjugation length. These polymers exhibit smaller band gaps, better ordering, and crystallinity in their solid states with improved electroconductivities. Moreover, exotic polymer architectures are excellent models to obtain deeper insight into the nature of electronic properties of conjugated systems.

Among conjugated polymers polythiophenes are one of the most promising and studied conjugated systems due to their synthetic availability, stability in various redox states, processability, and tunable electronic properties.[3] As a result these are promising candidates for molecular electronic devices.[4−6]

Cyclic oligothiophenes[7] and cyclic oligopyrroles[8] have recently been prepared. A few works were published describing these novel molecules and exploring their physical properties.[9] They show excellent self-assembling properties on substrates[10] and form unique 1:1 π-donor−π-acceptor complexes with C_{60} fullerenes.[11] In a recent paper, cyclic oligothiophenes were studied theoretically, revealing that cyclic polythiophenes were excellent models for linear polythiophenes.[12]

In chemical topology[13] the object is a molecule or a molecular assembly which is schematically represented on paper as a graph. If the graph contains crossings, then the graph and the molecule are referred to as nonplanar and topologically nontrivial, respectively. Figure 1 shows examples of both nonplanar (**I** and **II**) and planar (**III**) graphs. They are simplified projections of the enantiomers of the trefoil knot and a cycle, respectively. In [2]-catenane (**IV**), which represents a simplest
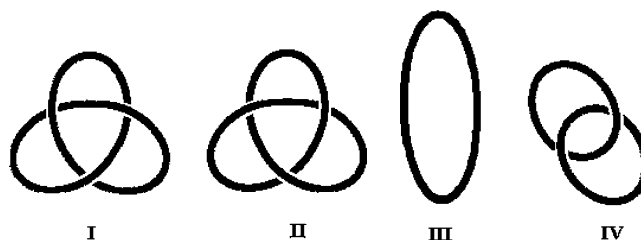

Figure 1. Simplified projections of the enantiomers of the trefoil knot (**I**, **II**), a cycle (**III**), and a [2]catenane (**IV**).

link, two cyclic molecules are mechanically linked with each other. The disruption of a catenane into its separate components requires the breaking of one or more covalent bonds in the mechanically linked molecule. Thus, catenanes behave as well-defined molecular compounds with properties significantly different from those of their individual components. A very elegant synthetic approach to the first fully conjugated thiophene containing catenanes[14] has been shown in a recent work, taking the molecular complexity of conjugated systems to the next level.

Oligothiophene [2]-catenanes and knots containing up to 28 thiophene units have been studied at BHandHLYP/3-21G* level of theory as the first attempt to predict the electronic properties of these exotic molecules.[15] We found that small knots (less than 22 thiophene units), and [2]-catenanes (less than 18 thiophene units) are extremely strained molecules. Larger knots and [2]-catenanes are almost strain-free and could be an attractive synthetic target. Vertical ionization potentials of knots and catenanes were always higher compared to lineal oligomers because of less effective conjugation.

This work is the first attempt to explore the electronic structure of mono and diionized states of oligothiophene catenanes and knots and compares them with those of linear oligomers. In case of linear polythiophenes, various theoretical studies[16] showed that for sufficiently long chains (longer than
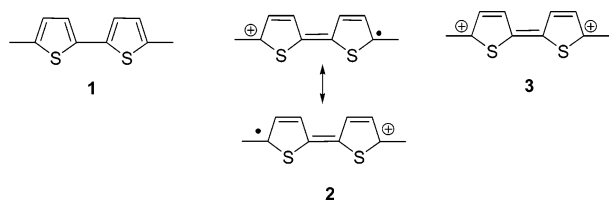
Oligothiophene Catenanes and Knots

J. Phys. Chem. A, Vol. 111, No. 16, 2007 **3125**

Figure 2. Valence structures representing neutral (**1**), monoionized (**2**), and diionized (**3**) fragments of polythiophene chain.

8−10 units), polarons are the most stable charged defects. A bipolaron tends to dissociate to a polaron pair when polymer chain is long enough. Although bipolaron is intrinsically stable

as shown in,[16c,16d] it is unstable with respect to the dissociation to a polaron pair. Bipolaron defects tend to stabilize and their localization increases when counterions are taken into account.[17]

Computational Details

Linear and cyclic oligomers are denoted as **Tn** and **Cn**, respectively, where **n** is the number of thiophene units. [2]-Catenanes and trefoil knots are denoted as **CATn** and **KNOTn**. Mono and diionized molecules are referred to as + and +2 (+2-**T** and +2-**S**), where **S** and **T** correspond to the singlet and triplet, respectively. Catenanes and knots containing 16, 22, and 28 thiophene units were selected for calculations
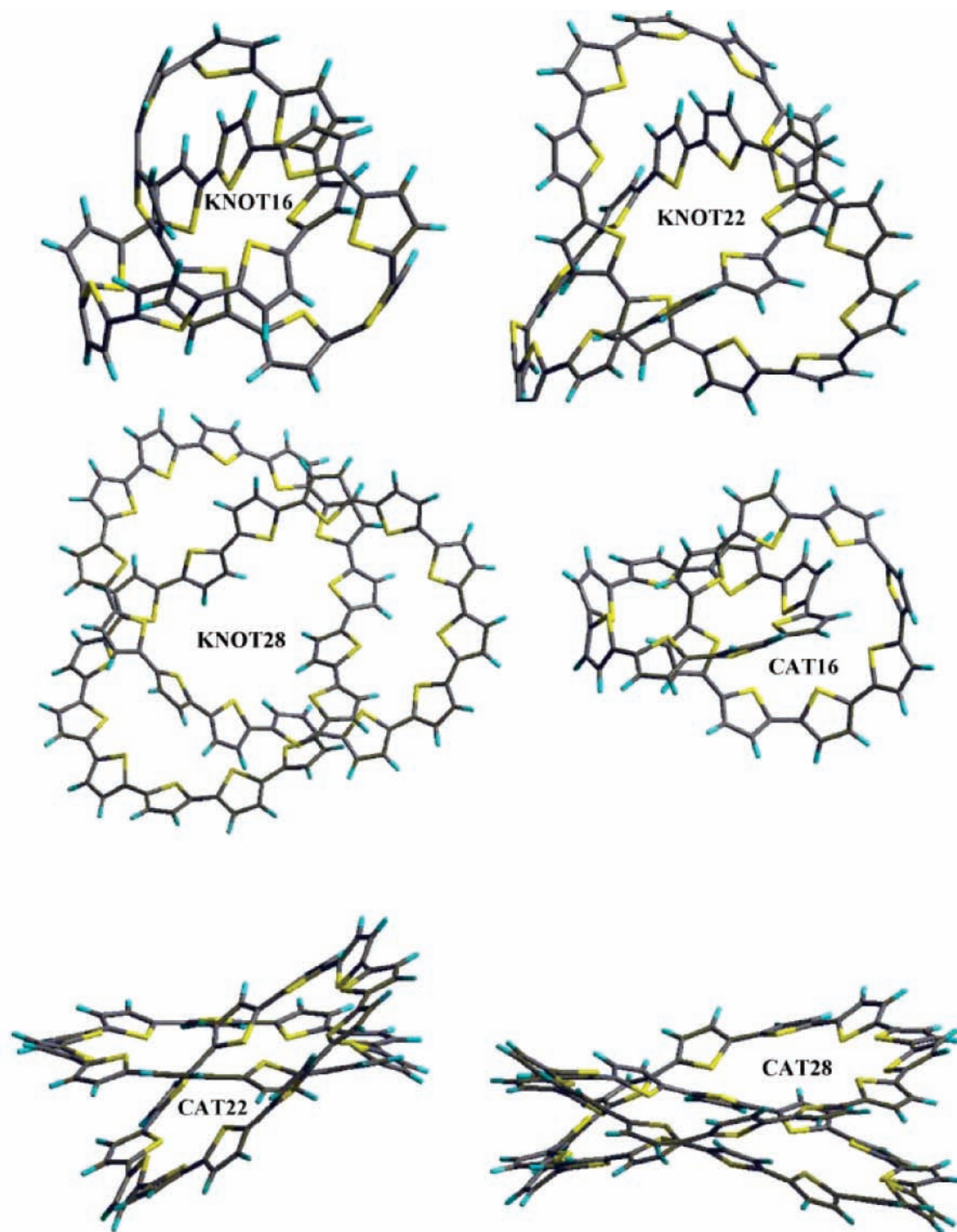

Figure 3. BHandHLYP/3-21G* optimized geometries of neutral catenanes and knots molecules.

representing small, medium and large molecules, respectively. The computational methodology is described in detail in our previous work.[15]

Neutral molecules were studied using restricted closed-shell Hartree−Fock formalism; cation radicals and dications were treated at unrestricted level. It has been shown that UDFT results are in very good agreement with CAS for conjugated systems when hybrid functionals are used.[18] All geometry optimizations were carried out with BHandHLYP hybrid functional as defined in Gaussian 03 package[19] in combination with 3-21G* basis set. Jaguar 6.0 suit of programs[20] was used for all calculations. Since BHandHLYP definitions are different in Gaussian and Jaguar packages, the following set of keywords was used to define BHandHLYP functional in Jaguar; idft = −1; xhf = 0.5; xexl1 = 0.5; xexnl1 = 0.5; xcornl2 = 1.0.

First, extensive conformational searches have been carried out using mixed torsional/large scale low mode sampling algorithm incorporated in Macromodel 9.0 suite of program using OPLS-AA force field in the gas phase. Each conformational search included 10000 iterations. Obtained lowest-energy structures were then used in DFT optimizations without any symmetry restrictions. For cyclic structures (from **C7** to **C14**), the lowest-energy structures located by conformational search were all *syn* conformers in line with.[12] It has been shown by Karpfen, Choi, and Kertesz that the description of the torsional barrier around the C−C bond in bithiophene strongly depends on the level of theory and basis set employed.[18b] We tested the reliability of our model calculating the torsional barrier around C−C bond in 2,2′-bithiophene and comparing the results with more elaborated MP2 model. Our model (BHandHLYP/3-21G*) gives the activation energy of 2.0 kcal/mol, while MP2 model used in [18a] showed 1.6, 2.6, and 1.6 kcal/mol for 6-31G*, 6-31++G**, and 6-311G(2d,2p) basis sets, respectively, in good agreement with our calculations.

Results and Discussion

Monoionized Species. The first step in the oxidative doping of the conjugated polymer is the formation of a cation radical (polaron). Cationic species are responsible for the hole transport phenomenon by a hopping-type mechanism between adjacent molecules or chains accompanied by geometric relaxation.[21] The reliable information on the extension and location of the charged defects can be obtained from the geometric structure. The geometry changes related to charge self-localization primarily concern the bond-alternation pattern along the backbone. Neutral thiophene rings are characterized by a pronounced carbon−carbon bond-length alternation, which corresponds to the aromatic like valence bond structure **1** in Figure 2. On the other hand, charged oligomers tend to adopt a marked quinoid geometry corresponding to the valence-bond structures **2** and **3**. Basically, the distinction between aromatic and quinoid structures allows one to determine the location and extension of the defect. Figure 3 shows optimized geometries of studied neutral oligothiophene catenanes and knots. Table 1 shows the bond lengths in neutral, mono, and diionized oligothiophenes of different architectures. As can be seen, the bond lengths are very sensitive to the oxidation state of oligomers. While C−S bonds are practically insensitive to the ionization, all other bonds change bond lengths as a consequence of the electron loss.

C−C bond connecting thiophene units in oligomer is the most sensitive and can be used as an indicator of charged defect delocalization. By plotting the inter-ring bond length against the number of thiophene units, the delocalization of charged defect can be estimated.

TABLE 1: Bond Lengths (Å) in Neutral, Mono, and Diionized Thiophene Oligomers Calculated at BHandHLYP/3-21G* Level of Theory

oligomer	1	2	3	4
CAT16	1.453−1.466	1.723−1.743	1.362−1.370	1.422−1.438
CAT16+	1.408−1.466	1.729−1.741	1.363−1.406	1.381−1.431
CAT16+2-S-v	1.401−1.465	1.725−1.743	1.361−1.408	1.381−1.429
CAT16+2-S-g	1.391−1.463	1.722−1.749	1.362−1.421	1.371−1.431
CAT16+2-T	1.402−1.466	1.725−1.749	1.361−1.408	1.381−1.429
CAT22	1.444	1.730−1.734	1.365−1.368	1.418−1.421
CAT22+	1.444−1.405	1.725−1.735	1.365−1.397	1.387−1.422
CAT22+2-S-v	1.402−1.447	1.727−1.738	1.367−1.397	1.386−1.421
CAT22+2-S-g	1.398−1.444	1.730−1.736	1.406−1.364	1.380−1.422
CAT22+2-T	1.404−1.445	1.729−1.737	1.400−1.365	1.384−1.422
CAT28	1.442−1.445	1.731−1.735	1.365−1.368	1.415
CAT28+	1.406−1.445	1.727−1.738	1.398−1.364	1.381−1.417
CAT28+2-S-v	1.400−1.444	1.732.1.740	1.366−1.402	1.375−1.416
CAT28+2-S-g	1.399−1.445	1.731−1.737	1.365−1.405	1.374−1.417
CAT28+2-T	1.401−1.444	1.731−1.739	1.365−1.402	1.376−1.416
KNOT16	1.471−1.485	1.733−1.785	1.355−1.376	1.414−1.432
KNOT16+	1.433−1.520	1.735−1.783	1.365−1.409	1.369−1.432
KNOT16+2-S	1.405−1.522	1.732−1.769	1.359−1.429	1.365−1.432
KNOT16+2-T	1.405−1.519	1.732−1.778	1.363−1.423	1.373−1.434
KNOT22	1.447−1.455	1.725−1.742	1.363−1.371	1.414−1.454
KNOT22+	1.404−1.455	1.727−1.742	1.361−1.404	1.381−1.426
KNOT22+2-S	1.401−1.456	1.727−1.744	1.361−1.408	1.375−1.428
KNOT22+2-T	1.401−1.455	1.729−1.744	1.360−1.408	1.375−1.428
KNOT28	1.442−1.450	1.728−1.736	1.364−1.368	1.413−1.422
KNOT28+	1.403−1.452	1.725−1.742	1.361−1.404	1.381−1.426
KNOT28+2-S	1.398−1.450	1.729−1.741	1.364−1.404	1.376−1.423
KNOT28+2-T	1.398−1.447	1.728−1.739	1.364−1.405	1.374−1.424
T28[a]	1.437	1.736	1.368	1.413
T28+	1.430−1.440	1.717−1.737	1.357−1.373	1.406−1.421
T28+2-S	1.403−1.438	1.714−1.740	1.358−1.395	1.382−1.419
T28+2-T	1.403−1.438	1.714−1.740	1.358−1.395	1.382−1.419

[a] Central ring

Figure 4 shows the polaron delocalization in linear polythiophene oligomers and the corresponding catenanes and knots containing 16, 22, and 28 repeating units. Polarons in **KNOT16+** and **CAT16+** are confined to five repeating units, while in case of **T28+,** polarons are delocalized essentially over the entire oligomer chain. The polaron delocalization in knots and catenanes is clearly related to the planarity of polythiophene chain. In case of linear oligomers where dihedral angles between thiophene fragments are close to zero, polarons are delocalized over the entire chain. The maximum dihedral angle decreases with number of monomer units for both catenanes and knots (from 87.0° for **KNOT16** to 48.6° for **KNOT28** and from 74.4° to 41.4° for **CAT16** and **CAT28**, respectively). In case of catenanes polarons are localized over one macrocycle leaving the second one intact. The second macrocycle in catenanes stabilizes polarons located at first macrocycle as can be seen from the comparison of the first ionization potentials (**IP$_1$**) and Mulliken charge distributions in monoionized catenanes (Tables 2 and 3). Although polarons in catenanes are localized only at one macrocycle, the second one has positive charges of 0.04, 0.03, and 0.03 for **CAT16+**, **CAT22+**, and **CAT28+** cationradicals, respectively. The polarization of the second ring on ionization reduces **IP$_1$** of catenanes compared to the respective cyclic oligothiophenes and increases the binding between oligothiophene rings in ionized catenanes compared to the neutral ones due to additional ion-induced dipole interactions. Additional stabilization drops from **CAT16+** to **CAT28+** as can be seen from energy difference between **IP$_1$** of catenanes and the corresponding cyclic oligomers due to looser structure of larger catenanes.
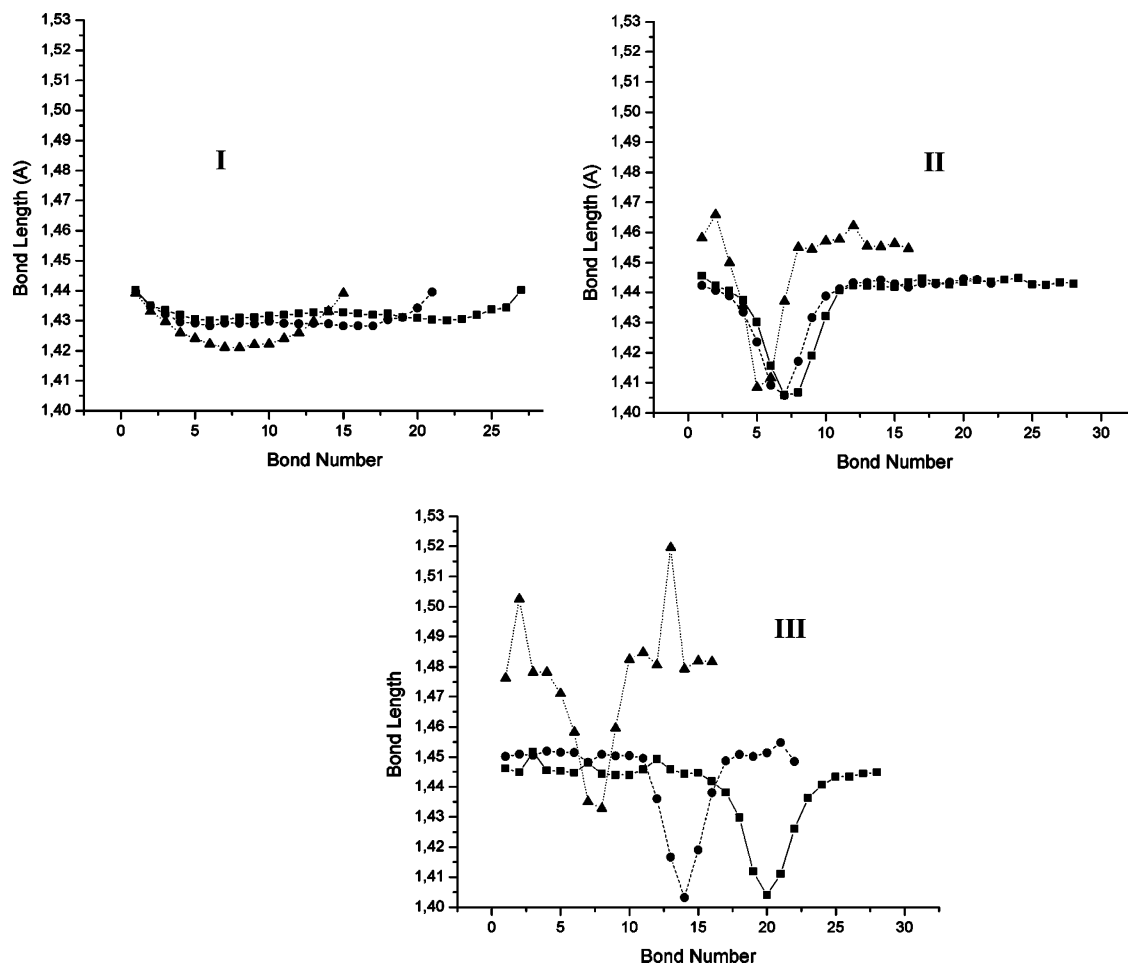
Oligothiophene Catenanes and Knots

J. Phys. Chem. A, Vol. 111, No. 16, 2007 **3127**

Figure 4. Inter-ring bond distances in monoionized linear oligomers (**I**), catenanes (**II**, and knots (**III**) containing 16 (▲), 22 (●), and 28 (■) thiophene repeating units, respectively.

TABLE 2: Adiabatic Ionization Potentials of Catenanes and Knots and Relaxation Energies Calculated at BHandHLYP/3-21G* Level (eV)

molecule	$IP_1{}^a$	$IP_2{}^b$	$\lambda_1{}^c$	$\lambda_2{}^d$
CAT16	5.85	7.79	0.42	0.86
CAT22	5.71	7.16	0.27	0.63
CAT28	5.64	6.88	0.31	0.65
KNOT16	5.93	7.93	0.28	0.31
KNOT22	5.74	7.33	0.28	0.39
KNOT28	5.78	6.84	0.21	0.44
C8	6.32	8.28	0.36	0.32
C11	6.01	7.50	0.23	0.26
C14	5.90	6.94	0.28	0.34
T8	6.03	7.77	0.18	0.17
T11	5.94	7.11	0.15	0.19
T14	5.90	6.69	0.11	0.20
T16	5.88	6.51	0.09	0.22
T22	5.84	6.25	0.07	0.20
T28	5.80	6.14	0.05	0.17

^{a} First adiabatic ionization potential. ^{b} Second adiabatic ionization potential. ^{c} Relaxation energy is the energy difference between the first vertical and adiabatic ionization potentials. ^{d} Relaxation energy is the energy difference between the second vertical and adiabatic ionization potentials

TABLE 3: Binding Energies (E_b) (kcal/mol) and Mulliken Charges in Neutral and Charged Catenane Molecules Calculated at BHandHLYP/3-21G* Level of Theory

catenane	$E_b{}^a$	$C_1{}^b$	$C_2{}^c$
CAT16	−11.3	0.00	0.00
CAT16+2-S-v	−36.5	1.00	1.00
CAT16+2-S-g	1.6	1.93	0.07
CAT16+2-T	−36.5	1.00	1.00
CAT16+	−0.6	0.96	0.04
CAT22	6.9	0.00	0.00
CAT22+2-S-v	−16.5	1.00	1.00
CAT22+-S-g	18.7	1.95	0.05
CAT22+2-T	−18.4	1.00	1.00
CAT22+	13.7	0.97	0.03
CAT28	9.3	0.00	0.00
CAT28+2-S-v	−11.5	1.00	1.00
CAT28+2-S-g	16.1	1.97	0.03
CAT28+2-T	−14.4	1.00	1.00
CAT28+	15.4	1.97	0.03

^{a} Binding energy calculated as the energy difference between the total energy of a catenane molecule and a sum of electronic energies of individual cycles in the corresponding charge state with opposite sign. ^{b} Mulliken charge at cycle 1 of a catenane. ^{c} Mulliken charge at cycle 2 of a catenane.

The relaxation energies are linearly related to the square root of the chain length for linear oligomers.[22] For cyclic oligothiophenes,[12] relaxation energies are larger compared to linear oligomers owing to greater geometry changes in cyclic cation radicals on ionization. In this work the relaxation energy was estimated as the energy difference between vertical and adiabatic ionization potentials.

A similar situation was found for catenanes and knots. As can be seen from Table 2, the relaxation energies of catenanes and knots are significantly higher compared to those of linear oligomers. There is a trend of reducing the relaxation energy with the number of thiophene units in catenanes and knots; nevertheless, even for **KNOT28+** and **CAT28+** molecules the relaxation energies are significantly higher compared to **T28+**.

TABLE 4: The Expectation Value of the S² Operator ⟨S²⟩ and the Relative Energies (*E*, kcal/mol) for the Open-Shell Singlet (Reference State), Triplet, and Closed-Shell Singlet Dicationic States (in Baskets) Calculated at BHandHLYP/3-21G* Level

molecule	E	⟨S²⟩
C8+2-S	0.0 (4.0)	1.03
C8+2-T	7.2	2.15
C11+2-S	0.0 (9.7)	1.36
C11+2-T	3.7	2.19
C14+2-S	0.0 (11.2)	1.54
C14+2-T	2.3	2.27
CAT16+2-S-v	0.0	1.28
CAT16+2-S-g	9.2 (10.5)	0.83
CAT16+2-T	0.0	2.28
CAT22+2-S-v	0.0	1.30
CAT22+2-S-g	2.8 (10.2)	1.35
CAT22+2-T	1.9	2.31
CAT28+2-S-v	0.0	1.38
CAT28+2-S-g	0.7 (10.5)	1.45
CAT28+2-T	2.9	2.39
KNOT16+2-S	0.0 (6.1)	1.49
KNOT16+2-T	−0.1	2.49
KNOT22+2-S	0.0 (10.8)	1.35
KNOT22+2-T	0.4	2.29
KNOT28+2-S	0.0 (14.5)	1.39
KNOT28+2-T	0.5	2.29
T8+2-S	0.0 (8.4)	1.23
T8+2-T	2.7	2.15
T11+2-S	0.0 (14.0)	1.22
T11+2-T	0.8	2.20
T14+2-S	0.0 (17.6)	1.29
T14+2-T	1.0	2.12
T16+2-S	0.0 (18.8)	1.37
T16+2-T	0.3	2.29
T22+2-S	0.0 (17.1)	1.35
T22+2-T	0.0	2.33
T-28 + 2-S	0.0 (14.4)	1.32
T28+2-T	0.0	2.32

In case of linear oligomers and knots, the relaxation energies reduce with polaron delocalization as can be seen from Figure 4 and Table 2. Thus, the delocalization of polarons is similar for **KNOT16+** and **KNOT22+**, and their relaxation energies are similar too. This is not the case for catenanes where second macrocycle participates in the stabilization of polarons increasing the relaxation energy compared to knots for **CAT16+** and **CAT28+**. In case of **CAT22+** and **KNOT22+**, the difference in polaron delocalization (five repeating units for **KNOT22+** and 8 for **CAT22+**) and the participation of second macrocycle in stabilization of polarons in **CAT22+** compensate one another in terms of the contribution to the relaxation energy.

When comparing **IP₁**'s of catenanes, knots, and linear oligomers, one can note three distinctive features (Table 2). First, similar to linear oligomers, **IP₁**'s for catenanes and knots decrease with the number of repeating units. Second, in case of knots, **IP₁**'s are similar for **KNOT22** and **KNOT28**. Third, **IP₁**'s of catenanes and knots are very much alike to those of linear oligomers with the same number of thiophene fragments due to higher relaxation stabilization of polarons specific to molecular architecture of catenanes and knots. As mentioned above, the second macrocycle in catenanes stabilizes polarons, reducing **IP₁**'s of catenanes compared to the corresponding single macrocycles from 0.47 eV for **CAT16** to 0.12 eV for **CAT28.** This effect represents a model of interchain interactions in ionized bulk polythiophene.

Diionized Species. It has been shown[12] that singlet RHF solution is unstable with respect to UHF one for linear and cyclic dicationic states of oligothiophenes. RHF solution corresponds to bipolaron defect, while UHF one corresponds to polaron pair.

When linear oligomer contains less that 6−8 repeating units, UHF solution is converged to RHF one reflecting the impossibility the of bipolaron dissociation. Our calculations confirmed this finding for catenanes and knots too. Moreover, RHF solution results in qualitatively wrong structure for diionized states of catenanes. Table 4 shows the relative energies for different spin states of dicationic defects in oligothiophenes of distinct architectures. As can be seen, the energy difference between RHF and UHF solutions for singlet states increases with the number of thiophene units reaching 18.8 kcal/mol for **T22**. The energies of open-shell singlets are similar or lower compared to triplet states. The difference reaches 7.2 kcal mol for **C8**, and the stability of triplet states increases with the number of thiophene units in cyclic, linear oligothiophenes, and oligothiophene knots. In case of linear oligothiophenes, open-shell singlet and triplet states become practically degenerate for **T22** and **T28,** corresponding to completely dissociated non interacting polaron pair.

In case of knot dications, both triplet and open-shell singlets are dissociated polaron pairs. It is seen from Figure 5 and Table 4 that the relative energies of triplet and open-shell singlet dicationic states are depended on the defect delocalization. In case of excessive confinement, the doubly charged defects are generally more localized in triplet state due to additional restriction imposed by Pauli repulsion, increasing the energy of such states. When comparing the singlet and triplet defects delocalization in **C8** where the triplet-open-shell singlet gap is the most pronounced (Figure 6), one can observe the difference. In both cases the shortest bonds (polaron centers) are separated by four thiophene units; however, the difference between shortest and longest bonds is of 0.040 Å for triplet and 0.014 Å for open-shell singlet defects, respectively, manifesting stronger localization of the former.

The properties of double ionized catenanes are markedly different from those of knots, cyclic and linear oligothiophenes due to the existence of two electronically independent units. The first difference is that two different singlet double ionized states were found for oligothiophene catenanes. When optimization is started from neutral catenane geometry, the resulting dication is **S-v**. However, when initial geometry for optimization is cation radical, the geometry is converged to a different minimum (**S-g**).

The difference between two minima is clearly seen from Figure 6. In the case of **S-v**, the polaron pair is distributed uniformly over two macrocycles, while in case of the **S-g** minimum, the polaron pair resides at one macrocycle. Similar conclusion can be made inspecting the Mulliken charge distribution for two different minima (Table 3). In **S-v**, each macrocycle has a positive charge of exactly +1, while in **S-g**, one macrocycle is almost neutral while the other is nearly doubly charged. As might be expected, **S-v** is more stable than **S-g** because of the polaron pair is completely dissociated. As can be seen from Figure 6 in the case of **CAT16+2-S-g,** dication polaron pairs are barely dissociated, while in **CAT22+2-S-g** and **CAT28+2-S-g**, the dication bipolaron pair is completely dissociated. As can be seen from Table 4, the dissociation extent of polaron pair in **S-g** defines the relative energy of **S-v** and **S-g** minima. This difference drops with the number of thiophene units in catenanes from 9.2 kcal/mol for **CAT16+2-S-g** to 0.7 kcal/mol for **CAT28+2-S-g**. Thus, in case of **CAT22** and **CAT28 S-g** minima are thermally reachable from **S-v** minimum and they can coexist. As can be seen from Table 4, the binding energy between catenane macrocycles in **S-v** is notoriously negative because of the electrostatic repulsion between polarons.
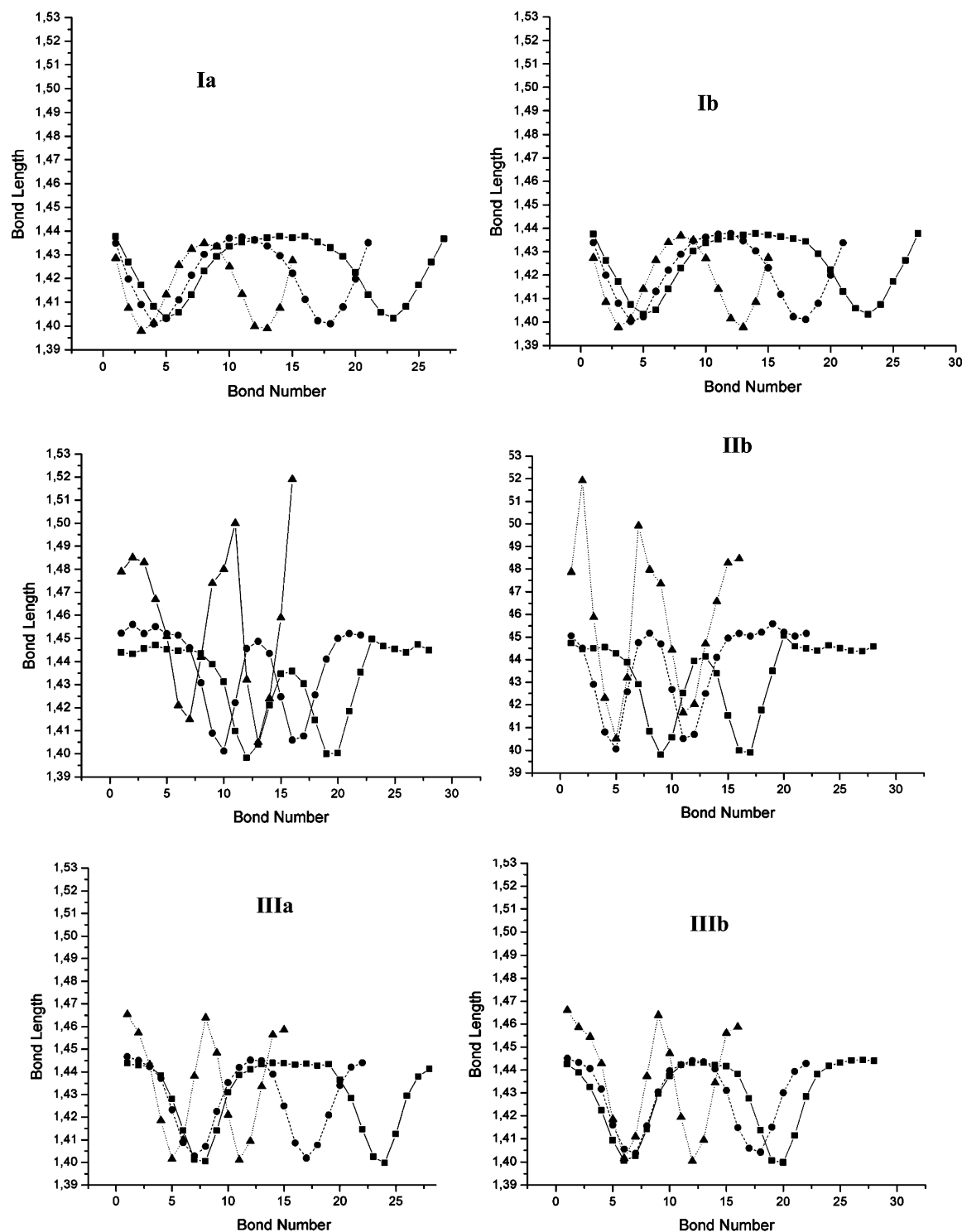
Oligothiophene Catenanes and Knots

J. Phys. Chem. A, Vol. 111, No. 16, 2007 **3129**

Figure 5. Inter-ring bond distances in diionized oligothiophene oligomers in singlet (**a**) and triplet (**b**) states; linear (**I**), catenanes (**II**), and knots (**III**) containing 16 (▲), 22 (●), and 28 (■) thiophene repeating units, respectively.

On the other hand, in **S-g** minima, the binding energy is more positive compared to neutral and even monoionized catenanes because of the strong ion-induced dipole interactions. Table 3 shows that induced charge at second catenane ring is more positive for the **S-g** minimum compared to cation-radicals.

Similar to cyclic, linear oligothiophenes, and oligothiophene knots, the open-shell singlet state for catenanes is more stable than corresponding triplet. The difference, however, is rather small (Table 4) and does not depend on the number of repeating units as for other studied molecular architectures. Unlike singlets, the only triplet state was detected for doubly ionized

catenanes where each macrocycle has one polaron independently of starting geometry chosen for the optimization.

There is a marked difference between conformations of singlet and triplet states of double ionized catenanes, which is most notorious for the **CAT22** dication (Figure 7). As can be seen, the macrocycles are almost perpendicular to each other in triplet state, while this angle is about 30° for the open-shell singlets. This difference is due to the Pauli repulsion existing in triplet state. Unpaired electrons are located at π orbitals perpendicular to the macrocycle planes; therefore, the overlap is minimal when macrocycles are perpendicular to each other, thus decreasing
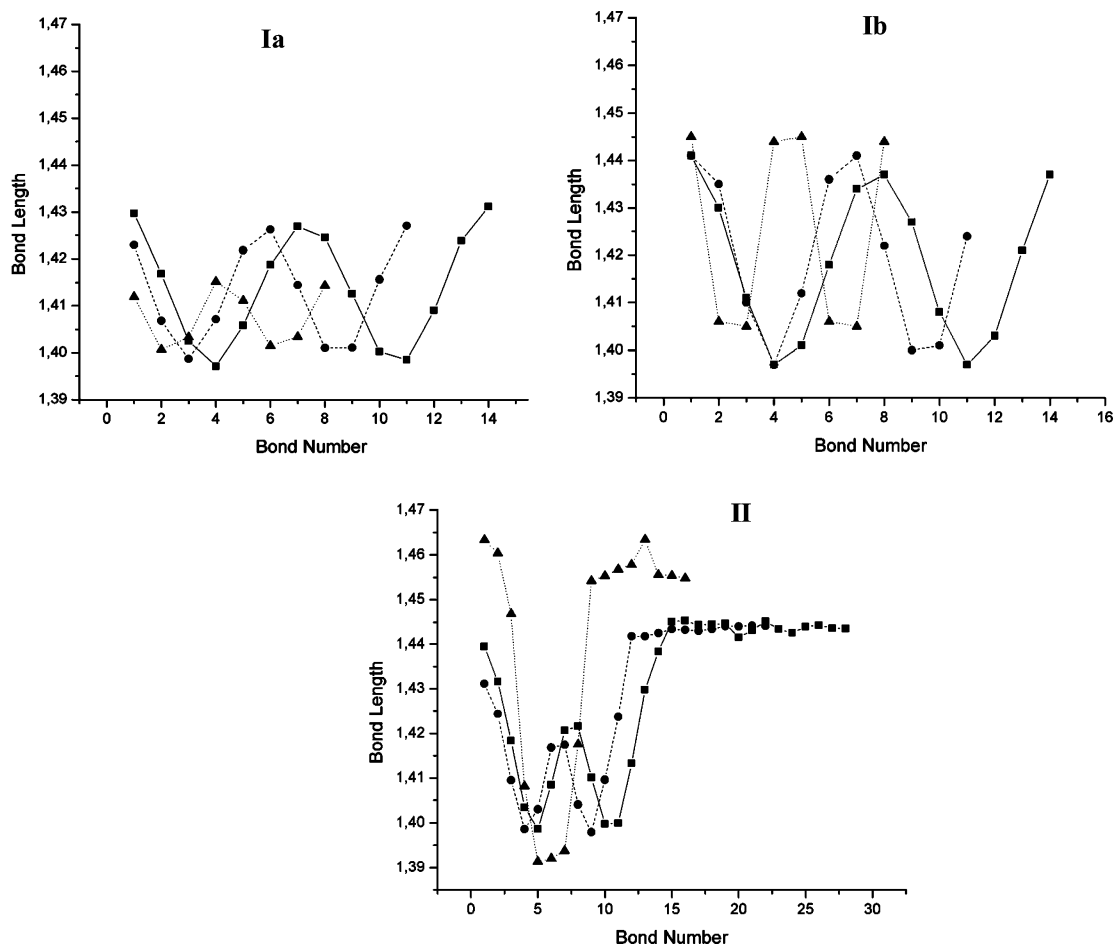
Figure 6. Inter-ring bond distances in singlet (**Ia**) and triplet (**Ib**) dicationic states of cyclic oligothiophenes and **S-g** state of oligothiophene catenanes (**II**) containing 16 (▲), 22 (●) and 28 (■) thiophene repeating units, respectively.
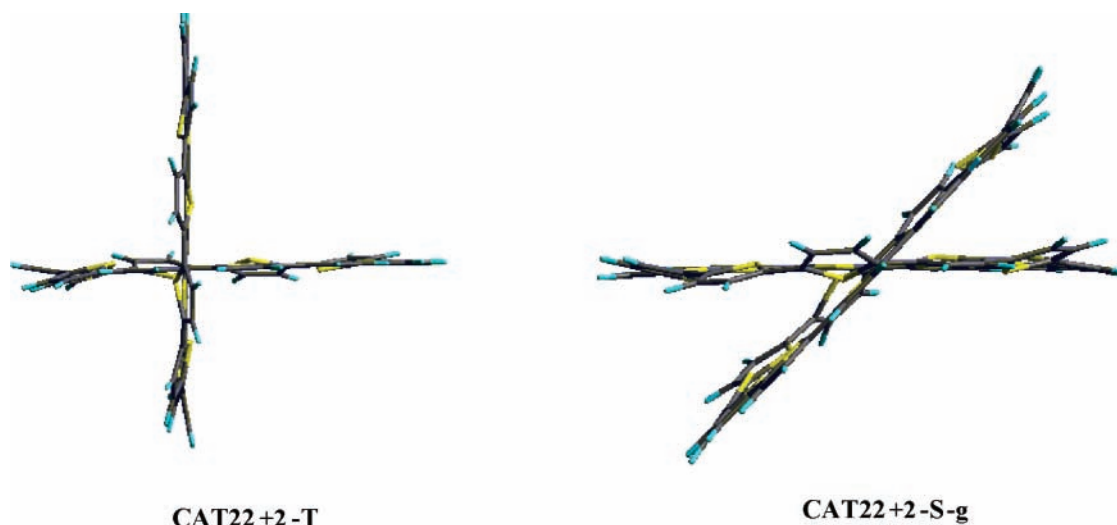

Figure 7. BHandHlyp/3-21G* optimized geometries of **CAT22+2-T** and **CAT22+2-S-v** molecules.

the Pauli repulsion between unpaired electrons. In case of **CAT16** and **CAT28** dications, this effect is not so pronounced. In **CAT16**, mutual movements of two macrocycles are strongly hindered. In **CAT28** there is very little overlapping between orbitals of the macrocycles due to macrocycles size.

Table 2 shows second adiabatic ionization potentials of studies molecules (**IP$_2$**). As can be seen, the difference between **IP$_1$** and **IP$_2$** decreases with the number of repeating units for all types of oligomers reflecting increasing dissociation of polaron pair in large oligomers. This difference is largest for knots and

catenanes reaching about 2 eV for **CAT16** and **KNOT16** and smallest for large linear oligomers (0.34 eV for **T28**). Unlike **IP$_1$**, **IP$_2$** depends on the molecular architecture. Linear oligomers show smallest **IP$_2$**'s, followed by knots and catenanes. As can be seen, for all types of oligomers, λ_2 is larger than λ_1. This difference can be rationalized in terms polaron localization in dications due to electrostatic repulsion. This fact can be evidenced inspecting Figures 4−6. Interestingly, λ_2 does not obey the trend found for λ_1 for linear oligothiophenes.[22] According to this explanation, the difference between λ_2 and

Oligothiophene Catenanes and Knots

J. Phys. Chem. A, Vol. 111, No. 16, 2007 **3131**

λ_1 must increase with delocalization of polaron in monocations. Indeed, λ_2 is 3 times λ_1 for **T22** and **T28**, where polarons are highly delocalized, while for short linear oligomers, cycles, and knots, where polarons are confined to 5−8 units, λ_2 is similar to λ_1. In the case of catenanes, λ_2 is twice λ_1 and twice λ_2 for cyclic oligomers due to the participation of the second macrocycle in stabilization of dication. Thus, as can be seen from Figures 4−6, the delocalization of polarons is less pronounced in diionized molecules compared to monoionized ones.

Conclusions

The delocalization of polarons is related with the planarity of oligothiophene chain. Thus, the polaron delocalization is largest in linear oligomers and smallest in catenanes and knots. In all cases polaron delocalization increases with the number of thiophene units; however, for knots and catenanes containing 22 and 28 thiophene fragments, the polaron delocalization differs only slightly. The relaxation energy (λ_1) increases with polaron localization. In case of catenane cation radicals, polarons are localized at one macrocycle leaving another one intact. **IP$_1$** of studied molecules depends mostly on the number of thiophene units, not on the molecular architecture

A polaron pair, not a bipolaron, is the most stable dicationic state for all studied molecules. A singlet polaron pair is more stable than a triplet one. The energy difference between triplet and singlet states does not exceed 7−8 kcal/mol and decreases with the number of thiophene units in oligomer. Two different singlet minima were found for diionized catenanes. In the first one (the most stable), each macrocycle loses one electron and in the other a polaron pair is located at one. The energy difference between two minima decreases with the number of units in catenane, reaching only 0.7 kcal/mol for **CAT28** dication. Each macrocycle has only one polaron in the triplet state

Unlike **IP$_1$**, **IP$_2$** is smallest for linear oligomers, followed by catenanes and knots. The linear dependence of the relaxation energy on the square root of the chain length of the linear oligomers is not obeyed for the second ionization process.

Supporting Information Available: Cartesian coordinates. This material is available free of charge via the Internet at http://pubs.acs.org.

References and Notes

(1) (a) Prosa, T. J.; Winokur, M. J.; McCullough, R. D. *Macromolecules* **1996**, *29*, 3654. (b) McCullough, R. D. *Adv. Mater.* **1998**, *10*, 93. (c) Chen, T. A.; Wu, X.; Rieke, R. D. *J. Am. Chem. Soc.* **1995**, *117*, 233.

(2) Bao, Z.; Dodabalapur, A.; Lovinger, A. J. *Appl. Phys. Lett.* **1996**, *69*, 4108.

(3) Fichou, D. Ed. *Handbook of Oligo and Polythiophenes*; Wiley-VCH: Weinheim, Germany, 1999.

(4) . (a) Horowitz, G.; Peng, X.; Fichou, D.; Garnier, F. *J. Appl. Phys.* **1990**, *67*, 528. (b) Paloheimo, J.; Kuivalainen, P.; Stubb, H.; Vuorimaa, E.; Yli-Lahti, P. *Appl. Phys. Lett.* **1990**, *56*, 1157.

(5) (a) Perepichka, I. F.; Perepichka, D. F.; Meng, H.; Wudl, F. *Adv. Mater.* **2005**, *17*, 2281. (b) Geiger, F.; Stoldt, M.; Schweizer, H.; Baüerle, P.; Umbach, E. *Adv. Mater.* **1993**, *5*, 922.

(6) (a) Brabec, C. J.; Sariciftci, N. S.; Hummelen, J. C. *Adv. Funct. Mater.* **2001**, *11*, 15. (b) Hoppe, H.; Sariciftci, N. S. *J. Mater. Res.* **2004**, *19*, 1924.

(7) (a) Fuhrmann, G.; Debaerdemaeker, T.; Bäuerle, P. *Chem. Commun.* **2003**, 948. (b) Krömer, J.; Rios-Carreras, I.; Fuhrmann, G.; Musch, C.; Wunderlin, M.; Dabaerdemaeker, T.; Mena-Osteritz, E.; Bäuerle, P. *Angew. Chem., Int. Ed.* **2000**, *39*, 3481.

(8) (a) Seidel, D.; Lynch, V.; Sessler, J. L. *Angew. Chem., Int. Ed.* **2002**, *41*, 1422. (b) Köhler, T.; Seidel, D.; Lynch, V.; Arp, F. O.; Ou, Z.; Kadish, K. M.; Sessler, J. L. *J. Am. Chem. Soc.* **2003**, *125*, 6872. (c) Gorski, A.; Koehler, T.; Seidel, D.; Lee, J. T.; Orzanowska, G.; Sessler, J. L.; Waluk, J. *Chem. Eur. J.* **2005**, *11*, 4179.

(9) (a) Bednarz, M.; Rwineker, P.; Mena-Osteritz, E.; Bäuerle, P. *J. Lumin.* **2004**, *110*, 225. (b) Casado, J.; Hernández, V.; Ponce Ortiz, R.; Ruiz Delgado, M. C.; L'opez, Navarrete, J. T.; Fuhrmann, G.; Bäuerle, P. *J. Raman Spectrosc.* **2004**, *35*, 592.

(10) (a) Mena-Osteritz, E.; Bäuerle, P. *Adv. Mater.* **2001**, *13*, 243. (b) Mena-Osteritz, E. *Adv. Mater.* **2002**, *14*, 609.

(11) Mena-Osteritz, E.; Bäuerle, P. *Adv. Mater.* **2006**, *18*, 447.

(12) Sanjio, S. Z.; Bendikov, M. *J. Org. Chem.* **2006**, *71*, 2972.

(13) (a) Frisch, H. L.; Wasserman, E. *J. Am. Chem. Soc.* **1961**, *83*, 3789. (b) Chambron, J.-C.; Dietrich-Buchecker, C.; Sauvage, J.-P. *Top. Curr. Chem.* **1993**, *165*, 132.

(14) Ammann, M.; Rang, A.; Schalley, C. A.; Bäuerle, P. *Eur. J. Org. Chem.* **2006**, 1940.

(15) Fomine, S.; Guadarrama, P. *J. Phys. Chem. A* **2006**, *110*, 10098.

(16) (a) Gao, Y.; Liu, C.-G.; Jiang, Y.-S. *J. Phys. Chem. A* **2002**, *106*, 5380. (b) Geskin, V. M.; Brédas, J. L. *Chem. Phys. Chem.* **2003**, *4*, 498. (c) Ehrendorfer, C.; Karpfen, A. *J. Phys. Chem.* **1995**, *99*, 5341. (d) Ehrendorfer, C.; Karpfen, A. *J. Phys. Chem.* **1994**, *98*, 7492.

(17) (a) Irle, S.; Lischka, H. *J. Chem. Phys.* **1997**, *107*, 3021. (b) Irle, S.; Lischka, H. *J. Mol. Struct. (THEOCHEM)* **1996**, *364*, 15.

(18) (a) Bendikov, M.; Duong, H. M.; Starkey, K.; Houk, K. N.; Carter, E. A.; Wudl, F. *J. Am. Chem. Soc.* **2004**, *126*, 7416. (b) Karpfen, A.; Choi, C.-H.; Kertesz, M. *J. Phys. Chem. A* **1997**, *101*, 7426.

(19) Frisch, M. J.; Trucks, G. W.; Schlegel, H. B.; Scuseria, G. E.; Robb, M. A.; Cheeseman, J. R.; Montgomery, J. A., Jr.; Vreven, T.; Kudin, K. N.; Burant, J. C.; Millam, J. M.; Iyengar, S. S.; Tomasi, J.; Barone, V.; Mennucci, B.; Cossi, M.; Scalmani, G.; Rega, N.; Petersson, G. A.; Nakatsuji, H.; Hada, M.; Ehara, M.; Toyota, K.; Fukuda, R.; Hasegawa, J.; Ishida, M.; Nakajima, T.; Honda, Y.; Kitao, O.; Nakai, H.; Klene, M.; Li, X.; Knox, J. E.; Hratchian, H. P.; Cross, J. B.; Bakken, V.; Adamo, C.; Jaramillo, J.; Gomperts, R.; Stratmann, R. E.; Yazyev, O.; Austin, A. J.; Cammi, R.; Pomelli, C.; Ochterski, J. W.; Ayala, P. Y.; Morokuma, K.; Voth, G. A.; Salvador, P.; Dannenberg, J. J.; Zakrzewski, V. G.; Dapprich, S.; Daniels, A. D.; Strain, M. C.; Farkas, O.; Malick, D. K.; Rabuck, A. D.; Raghavachari, K.; Foresman, J. B.; Ortiz, J. V.; Cui, Q.; Baboul, A. G.; Clifford, S.; Cioslowski, J.; Stefanov, B. B.; Liu, G.; Liashenko, A.; Piskorz, P.; Komaromi, I.; Martin, R. L.; Fox, D. J.; Keith, T.; Al-Laham, M. A.; Peng, C. Y.; Nanayakkara, A.; Challacombe, M.; Gill, P. M. W.; Johnson, B.; Chen, W.; Wong, M. W.; Gonzalez, C.; Pople, J. A. *Gaussian 03*, revision B.04; Gaussian, Inc.: Pittsburgh, PA, 2003.

(20) *Jaguar 6.0*; Schrodinger, LLC: Portland, OR, 2005.

(21) (a) Brédas, J. L.; Calbert, J. P.; da Silva, D. A.; Cornil, J. *Proc. Natl. Acad. Sci. U.S.A.* **2002**, *99*, 5804. (b) Cornil, J.; Beljonne, D.; Calbert, J. P.; Brédas, J. L. *Adv. Mater.* **2001**, *13*, 1053.

(22) Hutchison, G. R.; Ratner, M. A.; Marks, T. J. *J. Am. Chem. Soc.* **2005**, *127*, 2339.